J|A|C|S
ARTICLES
Published on Web 02/25/2004

Dynamics of Positive Charge Carriers on Si Chains of Polysilanes

Shu Seki,* Yoshiko Koizumi, Tomoyo Kawaguchi, Hidefumi Habara, and Seiichi Tagawa*

Contribution from the Institute of Scientific and Industrial Research, Osaka University, 8-1 Mihogaoka, Ibaraki, Osaka 567-0047, Japan

Received November 28, 2003; E-mail: seki@sanken.osaka-u.ac.jp; tagawa@sanken.osaka-u.ac.jp

Abstract: The transient absorption of radical cations of a variety of substituted polysilanes is discussed quantitatively in terms of the molar extinction coefficient and oscillator strength by nanosecond pulse radiolysis. Oxygen-saturated polysilane solutions in benzene exhibit a strong transient absorption band ascribed to the polysilane radical cation. The transient species react with *N*,*N*,*N*′,*N*′-tetramethyl-*p*-phenylenediamine (TMPD) to produce TMPD radical cations. On the basis of the molar extinction coefficient of the TMPD radical cation, the molar extinction coefficients for the radical cations of polysilanes are found to increase in the range 3.3×10^4 to 2.0×10^5 M^{-1} cm^{-1} with increasing polymer segment length. The stepwise increase in the total oscillator strength with an increase in the number of phenyl rings directly bonded to the Si skeleton suggests the delocalization of the positive polaron state and/or the SOMO state over the phenyl rings, indicating the importance of phenyl rings in intermolecular hole transfer processes.

Introduction

Polysilanes bearing saturated Si backbones are of current interest because of their characteristic electron delocalization along the Si chain (σ-conjugated system[1]) and associated near-UV absorption,[2] photodecomposition,[3] and nonlinear optical properties.[4] On the basis of their utility as positive charge conductors, the dynamics of excess electrons and holes on the Si skeletons have been investigated vigorously in view of their potential application in electroluminescent diodes and as photoconductors.[5,6] The dominant process of charge carrier transport in polysilanes is the hopping of holes between localized states originating from domain-like subunits along the Si chain.[7,8] The mean length of the segments is controlled by steric hindrance of the side chains, thermal molecular motion, or both. Several groups have reported the synthesis of a series of polysilanes with backbone conformations varying from random coil to stiff and rodlike by changing the polymer substitution pattern.[9] Recently, Fujiki developed optically active polysilanes with tightly locked rodlike helical Si backbones achieved by the incorporation of chiral substituents.[10] The screw sense of the Si backbone was subsequently inverted by thermal treatment in diarylpolysilanes with chiroptical switching of the main chain chromophores, indicating the highly ordered backbone conformations of these polymers.[11]

Despite positive charge being the dominant charge carriers in the transport process, there have been few dynamics or quantitative analyses on the electronic state of positive charges on the Si chain other than by transient spectroscopy[12,13] or electron spin resonance.[14,15] Localization of the charge carriers was revealed to be suppressed in the polysilanes bearing bulky pendant groups, suggesting not only that the localization in typical dialkyl polysilanes arises from the flexibility of Si catenation, but also that delocalization occurs in polysilanes with stiff or rodlike Si skeletons. However, the quantitative correlation between the molecular stiffness and the degree of positive charge delocalization had not been elucidated to date.

The present paper reports on the direct observation of polysilane radical cations by pulse radiolysis. Pulse-radiolysis transient absorption spectroscopy (PR-TAS) is a very powerful and useful technique for achieving the selective formation of radical ions in matrixes (solvents) and tracing reaction kinetics. To date, quantitative tracing of polysilane radical cations has been very difficult because of their very low ionization potentials (<6 eV)[16,17] and complicating side reactions. Recent improvements in our transient spectroscopy system have made it possible

(1) Rice, M. *J. Phys., Lett.* **1979**, *71A*, 152.
(2) West, R. *J. Organomet. Chem.* **1986**, *300*, 327.
(3) Trefonas, P.; West, R.; Miller, R. D. *J. Am. Chem. Soc.* **1985**, *107*, 2737.
(4) Kajzar, F.; Messier, J.; Rosilio, C. *J. Appl. Phys.* **1986**, *60*, 3040.
(5) Kepler, R. G.; Zeigler, J. M.; Harrah, L. A.; Kurtz, S. R. *Phys. Rev.* **1987**, *B35*, 2818.
(6) Suzuki, H.; Meyer, H.; Hoshino, S.; Haarer, D. *J. Lumin.* **1996**, *66*−*67*, 423.
(7) Fujino, M. *Chem. Phys. Lett.* **1987**, *136*, 451.
(8) Abkowitz, M.; Knier, F. E.; Yuh H. J.; Weagley, R. J.; Stolka, M. *Solid State Commun.* **1987**, *62*, 547.
(9) Fujiki, M. *J. Am. Chem. Soc.* **1996**, *118*, 7424.
(10) Fujiki, M. *J. Am. Chem. Soc.* **1994**, *116*, 6017.
(11) Koe, J. R.; Fujiki, M.; Nakashima, H.; Motonaga, M. *Chem Commun.* **2000**, 389.
(12) Ban, H.; Sukegawa, K.; Tagawa, S. *Macromolecules* **1987**, *20*, 1775.
(13) Ban, H.; Sukegawa, K.; Tagawa, S. *Macromolecules* **1988**, *21*, 45.
(14) Kumagai, J.; Yoshida, H.; Ichikawa, T. *J. Phys. Chem.* **1995**, *99*, 7965.
(15) Seki, S.; Cromack, K. R.; Trifunac, A. D.; Yoshida, Y.; Tagawa, S.; Asai, K.; Ishigure, K. *J. Phys. Chem. B* **1998**, *102*, 8367.
(16) Seki, K.; Mori, T.; Inokuchi, H.; Murano, K. *Bull. Chem. Soc. Jpn.* **1988**, *61*, 351.
(17) Ishii, H.; Yuyama, A.; Norioka, S.; Seki, K.; Hasegawa, S.; Fujino, M.; Isaka, H.; Fujiki, M.; Matsumoto, N. *Synth. Met.* **1995**, *69*, 595.

10.1021/ja039840e CCC: $27.50

Table 1. Substitution Patterns and Molecular Weights of Polysilanes

entry	*R*1	*R*2	M_w[a]	M_n[b]	entry	*R*1	*R*2	M_w[a]	M_n[b]
PH1	CH_3	C_6H_5	5.5×10^4	4.8×10^4	PD8	*n*-C_8H_{17}	*n*-C_8H_{17}	1.4×10^6	6.8×10^4
PH2	C_2H_5	C_6H_5	3.4×10^4	1.5×10^4	PD10	*n*-$C_{10}H_{21}$	*n*-$C_{10}H_{21}$	6.1×10^5	1.7×10^5
PH3	*n*-C_3H_7	C_6H_5	5.2×10^4	2.4×10^4	PD12	*n*-$C_{12}H_{25}$	*n*-$C_{12}H_{25}$	1.4×10^6	5.2×10^5
PH4	*n*-C_4H_9	C_6H_5	2.0×10^4	1.1×10^4	ME3	C_3H_7	CH_3	0.91×10^5	1.5×10^4
PH5	*n*-C_5H_{11}	C_6H_5	1.7×10^6	8.0×10^5	ME4	C_4H_9	CH_3	1.0×10^5	0.96×10^4
PH6	C_6H_{13}	C_6H_5	4.6×10^6	1.1×10^6	ME5	C_5H_{11}	CH_3	1.0×10^5	1.6×10^4
PH7	C_7H_{15}	C_6H_5	2.1×10^5	8.9×10^4	ME6	C_6H_{13}	CH_3	0.85×10^5	1.0×10^4
PH8	C_8H_{17}	C_6H_5	5.2×10^6	1.8×10^6	ME8	C_8H_{17}	CH_3	5.5×10^5	3.5×10^4
PH10	*n*-$C_{10}H_{21}$	C_6H_5	8.8×10^5	4.0×10^5	ME10	$C_{10}H_{21}$	CH_3	1.9×10^5	2.8×10^4
PH12	*n*-$C_{12}H_{25}$	C_6H_5	4.2×10^5	1.4×10^5	ME12	$C_{12}H_{25}$	CH_3	0.87×10^5	2.1×10^4
PD4	*n*-C_4H_9	*n*-C_4H_9	7.8×10^5	2.8×10^5	PCHMS	C_6H_{11}	CH_3	4.9×10^5	1.8×10^5
PD5	*n*-C_5H_{11}	*n*-C_5H_{11}	1.1×10^6	4.1×10^4	DPA	*t*-C_4H_9−C_6H_5	*t*-C_4H_9−C_6H_5	3.2×10^5	1.1×10^5
PD6	*n*-C_6H_{13}	*n*-C_6H_{13}	1.1×10^6	5.1×10^5	DPB	*n*-C_4H_9−C_6H_5	*n*-C_4H_9−C_6H_5	6.1×10^5	1.5×10^5
PD7	*n*-C_7H_{15}	*n*-C_7H_{15}	1.9×10^6	9.4×10^5					

[a] Weight-average molecular weight. [b] Number-average molecular weight (determined relative to polystyrene).

to probe dilute solutions of transient species with a very high signal-to-noise (S/N) ratio.[18] This paper reports the molar extinction coefficient and oscillator strength of polysilane radical cations determined by both spectroscopic techniques and an efficient charge-transfer reaction between polysilane radical cations and *N*,*N*,*N*′,*N*′-tetramethyl-*p*-phenylene-diamine (TMPD). The degree of positive charge delocalization on Si chains is discussed in terms of the molecular stiffness of polysilanes, and the role of pendant phenyl rings in the charge carrier transport processes in polymer materials is addressed.

Experimental Section

General. Reagents and chemicals were purchased from Wako Chemical Co. unless otherwise stated. Nuclear magnetic resonance (NMR) spectra were collected using a JEOL EX-270 spectrometer for ^{1}H and ^{13}C spectra and using a Bruker ARX-400 spectrometer for ^{29}Si spectra, with chloroform-*d* as a solvent and tetramethylsilane as an internal standard. The molecular weight distribution of the obtained polymer was measured by gel permeation chromatography (GPC) using a Shimadzu LC-10Avp liquid chromatography system with tetrahydrofuran (THF) as an eluent and polystyrene calibration standards. The ultraviolet−visible (UV−vis) absorption spectra of the polysilanes in THF were recorded using a JASCO V-570 and a Shimadzu UV-3100PC. The photoluminescence spectra of Ar-saturated solutions were measured using a Perkin-Elmer LS-50B spectrophotometer.

Synthesis. All the monomers except for the compounds described below were purchased from Shin-Etsu Chemical Co. Ltd. and distilled twice prior to use. Polymerization was carried out by the Kipping method using R_1−R_2-dichlorosilanes with sodium metal in dry toluene for 5−20 h at 110 °C.[19] The polymer solution was precipitated in isopropyl alcohol (IPA) after filtration through a 0.45-mm PTFE filter to eliminate NaCl, and the precipitates were dried in a vacuum. The toluene solutions of the polymers were transferred into a separatory funnel, washed with water to eliminate remaining NaCl, and precipitated in IPA. The polymers were vacuum-dried at 80 °C and precipitated again in THF-methanol. The polymers were fractionally precipitated again to eliminate the lower molecular weight fraction of the bimodal distribution. The synthesized polymer entries and corresponding molecular weights are listed in Table 1, and the structures are schematized in Figure 1. The synthesis of poly[bis(*p*-*t*-butyl-phenyl)-silane] (DPA) and poly[bis(*p*-*n*-butyl-phenyl)silane] (DPB) are described elsewhere.[18]

Ethylphenyldichlorosilane (P2) and Propylphenyldichlorosilane (P3). A solution of ethylmagnesium bromide or *n*-propylmagnesium bromide in diethyl ether obtained by the reaction of ethylbromide or *n*-propylbromide with magnesium metal was cooled to −78 °C. Doubly distilled phenyltrichlorosilane purchased from Shin-Etsu Chemical Co. Ltd. was then added rapidly into the solution (1.0 equiv) and stirred for 2 h. The solution was slowly warmed to room temperature and refluxed for another 1 h. After rough filtration to remove MgBrCl, the solution was concentrated and distilled three times. The boiling points (bp) of P2 and P3 were 70 °C/5 Torr and 90 °C/5 Torr, respectively (yield: 52−60%). The polymerization of P2 and P3 gave PH2 and PH3 (yield: 32 and 28%). P2: ^{1}H NMR (270 MHz, $CDCl_3$), δ 1.14 (t, 3H, CH_3), 1.33 (q, 2H, CH_2), 7.41−7.54, (m, 3H, ArH), 7.70 (t, 2H, ArH). P3: ^{1}H NMR (270 MHz, $CDCl_3$), δ 1.02 (t, 3H, CH_3), 1.31−1.37 (m, 2H, CH_2−CH_3), 1.52−1.67 (m, 2H, Si−CH_2), 7.41−7.54 (m, 3H, ArH), 7.70−7.73 (m, 2H, ArH).

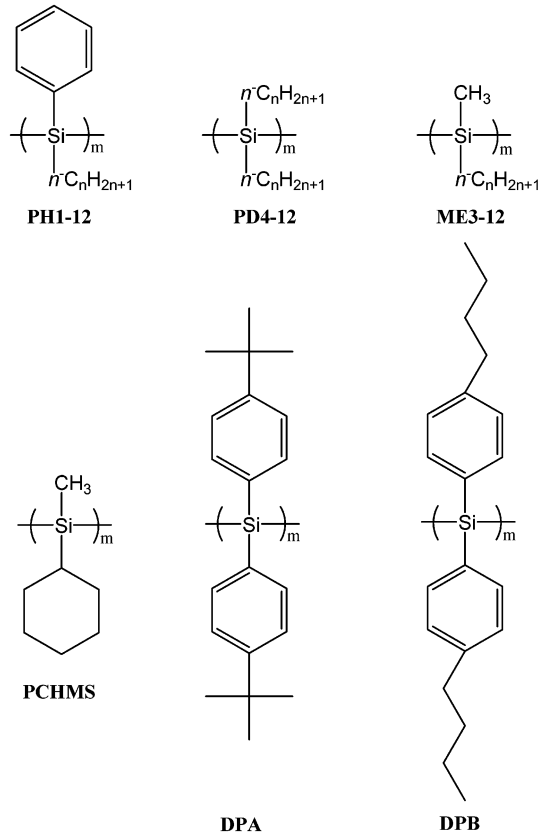

Figure 1. Structures of the series of polysilanes employed.

***n*-Butyl (P4), *n*-Pentyl (P5), *n*-Hexyl (P6), *n*-Heptyl (P7), *n*-Octyl (P8), *n*-Decyl (P10), and Dodecyl (P12) Phenyldichlorosilanes.** Solutions of *n*-alkylmagnesium bromide in THF were obtained by reaction of the corresponding *n*-alkylbromide with magnesium metal.

(18) Seki, S.; Matsui, Y.; Yoshida, Y.; Tagawa, S.; Koe, J. R.; Fujiki, M. *J. Phys. Chem. B* **2002**, *106*, 6849.
(19) Kipping, F. S. *J. Chem. Soc.* **1924**, *125*, 2291.

Phenyltrichlorosilane (1.2 equiv) was then added to the solution and stirred for 5 h. The solution was refluxed for another 2 h at 68 °C. After filtration, the solution was concentrated and distilled three times. The bp values were 104 °C/5 Torr (P4), 108 °C/5 Torr (P5), 120 °C/5 Torr (P6), 128 °C/5 Torr (P7), 136 °C/5 Torr (P8), 164 °C/5 Torr (P10), and 189 °C/5 Torr (P12) (yield: 65−70%). The polymerization of P4 and P12 gave PH4 and PH12 (yield: 7−22%). P4: ^{1}H NMR (270 MHz, $CDCl_3$), δ 0.90 (t, 3H, CH_3), 1.31−1.44 (m, 4H, CH_2), 1.47−1.59 (m, 2H, Si−CH_2), 7.42−7.55 (m, 3H, ArH), 7.70−7.74 (m, 2H, ArH). P5: ^{1}H NMR (270 MHz, $CDCl_3$), δ 0.86 (t, 3H, CH_3), 1.27−1.42 (m, 6H, CH_2), 1.45−1.58 (m, 2H, Si−CH_2), 7.42−7.54 (m, 3H, ArH), 7.70−7.75 (m, 2H, ArH). P6: ^{1}H NMR (270 MHz, $CDCl_3$), δ 0.87 (t, 3H, CH_3), 1.24−1.45 (m, 8H, CH_2), 1.49−1.58 (m, 2H, Si−CH_2), 7.39−7.51 (m, 3H, ArH), 7.69−7.73 (m, 2H, ArH). P7: ^{1}H NMR (270 MHz, $CDCl_3$), δ 0.87 (t, 3H, CH_3), 1.25−1.45 (m, 10H, CH_2), 1.49−1.60, (m, 2H, Si−CH_2), 7.41−7.53 (m, 3H, ArH), 7.70−7.73, (m, 2H, ArH). ^{13}C NMR (270 MHz, $CDCl_3$): 14.20 (CH_3), 20.80 (C^α, $^1J_{SiC}$ = 71 Hz), 22.56, 22.75, 28.86, 31.73, 32.47, 128.19, 131.40, 133.19, 133.23 ppm. ^{29}Si NMR (400 MHz, $CDCl_3$): 19.2 ppm. P8: ^{1}H NMR (270 MHz, $CDCl_3$), δ 0.87 (t, 3H, CH_3), 1.25−1.39 (m, 12H, CH_2), 1.48−1.57, (m, 2H, Si−CH_2), 7.41−7.53 (m, 3H, ArH), 7.70−7.73 (m, 2H, ArH). P10: ^{1}H NMR (270 MHz, $CDCl_3$), δ 0.86 (t,3 H, CH_3), 1.23−1.38 (m, 16H, CH_2), 1.47−1.59 (m, 2H, Si−CH_2), 7.40−7.53 (m, 3H, ArH), 7.69−7.72 (m, 2H, ArH). ^{13}C NMR (270 MHz, $CDCl_3$) 14.25 (CH_3), 20.79 (C^α, $^1J_{SiC}$ = 71 Hz), 22.55, 22.80, 29.18, 29.41, 29.54, 29.68, 29.83, 31.99, 32.51, 128.19, 131.40, 132.63, 133.22 ppm. ^{29}Si NMR (400 MHz, $CDCl_3$): 19.2 ppm. P12: ^{1}H NMR (270 MHz, $CDCl_3$), δ 0.88 (t, 3H, CH_3), 1.25−1.35 (m, 20H, CH_2), 1.49−1.54 (m, 2H, Si−CH_2), 7.37−7.50 (m, 3H, ArH), 7.68−7.72 (m, 2H, ArH). ^{13}C NMR (270 MHz, $CDCl_3$): 14.28 (CH_3), 20.81 (C^α, $^1J_{SiC}$ = 71 Hz), 22.58, 22.84, 29.20, 29.43, 29.58, 29.70, 29.85, 29.90, 29.93, 31.90, 32.54, 128.19, 131.40, 132.63, 133.22 ppm. ^{29}Si NMR (400 MHz, $CDCl_3$): 19.2 ppm.

Di-*n*-heptyl (D7), Di-*n*-octyl (D8), Di-*n*-decyl (D10), and Di-*n*-dodecyl (D12) Dichlorosilane. The corresponding *n*-alkyl-trichlorosilane (1.2 equiv) was rapidly added to the solutions of *n*-alkylmagnesium bromide in diethyl ether at 0 °C, allowed to warm to room temperature, and stirred for 12 h. The solution was refluxed for another 2 h. After filtration, the solution was concentrated and distilled three times. The bp were 142 °C/3 Torr (D7), 165 °C/3 Torr (D8), 190 °C/1 Torr (D10), and 195 °C/0.5 Torr (P12) (yield: 40−55%). The freezing points of D10 and D12 were 7 and 12 °C, respectively. The polymerization of D7 and D12 gave PD7 and PD12 (yield: 11−24%).

Pulse Radiolysis. All polysilanes were dissolved at 5 mM (base mol unit) in benzene (Bz) (spectroscopic grade from Dojin Chemical Co. Ltd.) or distilled 1-chlorobutane. O_2 was bubbled through the solutions for at least 5 min. After recrystallization in Bz, TMPD was added to the benzene solutions at concentrations of 0.098−0.37 mM.[20] The solutions were place into Suprasil quartz cells with a 2-cm optical path and irradiated with a single 8-ns electron pulse at room temperature. An Xe flash lamp was used as the source of light for analysis, with a continuous spectrum from 300 to 1600 nm. The analyzing light was monitored with a Ritsu MC-10N monochromator and detected by a PIN Si or InGaAs photodiode. The pulse radiolysis measurement was performed using an L-band electron linear accelerator at the Radiation Laboratory of the Institute of Scientific and Industrial Research, Osaka University. Dose per pulse was determined based on the $G\epsilon$ value of $(SCN)_2^-$ as 2.23×10^{-2} dm^2 J^{-1} for the irradiation of KSCN aqueous solution at 5.0×10^{-3} mol dm^{-3} concentrated, giving the value of dose per pulse in the present apparatus as 200−220 Gy. Other details of the apparatus are described elsewhere.[21] The typical instrument function was ca. 8 ns.

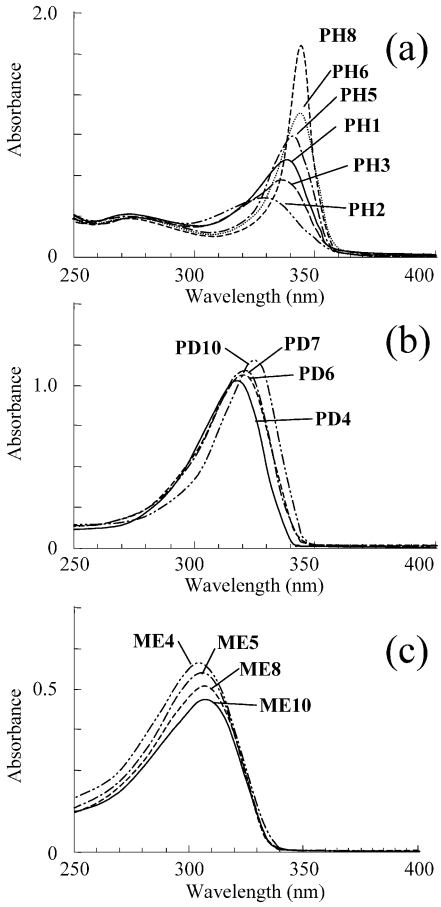

Figure 2. UV−vis absorption spectra of (a) poly(*n*-alkylphenylsilane)s, (b) poly(di-*n*-alkylsilane)s, and (c) poly(methyl-*n*-alkylsilane)s. Spectra were recorded at 25 °C for solutions of polysilanes in THF at 1.0×10^{-4} mol dm^{-3} (base mol unit).

Results and Discussion

The UV−vis absorption spectra of three series of polysilanes (*n*-alkylphenyl, di-*n*-alkyl, and methyl-*n*-alkyl substituted) are shown in Figure 2. The intense UV absorption band observed for steady-state polysilane solutions is ascribed to the transition between the valence band (VB) and the lowest excitonic states (ES) of the Si backbones.[22] The molar extinction coefficient (ϵ_{abs}) and oscillator strength (f_{VB-ES}) of the absorption are listed in Table 2. The values of both ϵ_{abs} and f_{VB-ES} depend strongly on the substitution patterns, with a considerable increase accompanying the change from asymmetric substitution (ME3-ME12) to symmetric (PD4-PD12). The values also increase dramatically with elongation of *n*-alkyl substituents from methyl to *n*-octyl in the case of poly(*n*-alkylphenylsilane)s, with only a slight drop with further elongation beyond *n*-octyl. Recently, Fujiki reported an empirical relationship between ϵ_{abs} and the viscosity index α, reflecting the geometric structure of the polymer main chain. The following empirical formula was obtained for the relationship between α and ϵ_{abs}:[9]

$$\epsilon_{abs} = 1130 \cdot e^{2.9\alpha} \quad (1)$$

The relationship between gyration length (R_g) and α is as follows:

(20) Stegman, J.; Cronkright, W. *J. Am. Chem. Soc.* **1970**, *92*, 6736.
(21) Seki, S.; Yoshida, Y.; Tagawa, S.; Asai, K. *Macromolecules* **1999**, *32*, 1080.
(22) Tachibana, H.; Kawabata, Y.; Koshihara, S.; Tokura, Y. *Solid State Commun.* **1990**, *75*, 5.

Table 2. UV Absorption, Fluorescence, and Optical Properties of Cation Radicals of Poly(*n*-alkylphenylsilane)s

entry	λ_{max}^{abs} (nm)	ϵ_{abs} [a]	f_{VB-ES} [b]	λ_{max}^{fl} (nm)	$\lambda_{max}^{\bullet+}$ (nm)	$\epsilon^{\bullet+}$ [c]	$f^{\bullet+}$	entry	λ_{max}^{abs} (nm)	ϵ_{abs} [a]	f_{VB-ES} [b]	λ_{max}^{fl} (nm)	$\lambda_{max}^{\bullet+}$ (nm)	$\epsilon^{\bullet+}$ [c]	$f^{\bullet+}$
PH1	339	7900	0.091	365	365	9.4	0.49	PD8	321	11 600	0.057	348	342	5.2	0.39
PH2	331	4300	0.0547	366	360	6.9	0.38	PD10	324	11 700	0.057	349	342	5.5	0.41
PH3	336	5700	0.0642	366	363	7.1	0.42	PD12	325	10 600	0.050	350	342	5.5	0.46
PH4	341	8000	0.0774	366	365	9.8	0.51	ME3	307	5200	0.043	338	348	3.8	0.24
PH5	342	9900	0.0914	367	369	12	0.59	ME4	306	6400	0.045	336	342	4.1	0.25
PH6	347	11 700	0.11	369	372	15	0.65	ME5	307	6100	0.045	336	346	4.5	0.28
PH7	348	14 300	0.11	369	372	16	0.59	ME6	307	5600	0.043	336	344	5.3	0.33
PH8	348	17 500	0.13	370	372	18	0.63	ME8	309	5500	0.041	336	338	4.5	0.32
PH10	348	16 600	0.13	369	370	17	0.66	ME10	310	5300	0.040	337	338	3.3	0.26
PH12	348	12 800	0.110	369	370	16	0.60	ME12	311	4700	0.034	336	342	3.5	0.24
PD4	317	10 400	0.053	346	346	4.5	0.31	PCHMS	326	7320	0.054	347	355	4.9	0.33
PD5	318	10 400	0.056	347	346	4.7	0.32	DPA	377	7600	0.0750		392[d]	17[d]	0.65[d]
PD6	319	10 600	0.056	347	344	5.1	0.37	DPB	393	13 300	0.11		<405[d]	>20[d]	>0.80[d]
PD7	321	10 900	0.057	348	340	5.2	0.38								

[a] Molar extinction coefficient per Si unit, in mol^{-1} dm^3 cm^{-1}. [b] Oscillator strength obtained by numerical integration. [c] Molar extinction coefficient per radical cation at the transient absorption maximum, in 10^4 mol^{-1} dm^3 cm^{-1}. [d] Data quoted from ref 18.

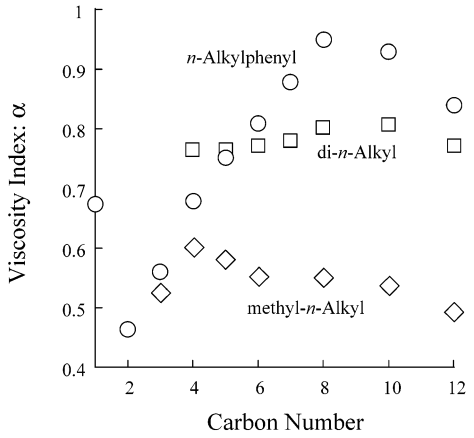

Figure 3. Viscosity index (α) of poly(*n*-alkylphenylsilane)s, poly(di-*n*-alkylsilane)s, and poly(methyl-*n*-alkylsilane)s as a function of length of *n*-alkyl substituents. Values of *a* are estimated from eq 1 based on ϵ_{abs}.

$$R_g = \kappa M^{\nu} \tag{2}$$

where κ is a constant, M is the molecular weight of the polymer, and $\nu = (\alpha + 1)/3$. The estimated values of α are shown in Figure 3; they vary from 0.46 for PH2 to 0.94 for PH8. Assuming a constant polymerization degree for the polysilanes, R_g is expected to increase with ϵ_{abs}. The actual Kuhn segment lengths (q) of the polymers were found to be $q = 1.1$ nm for PH1,[18] 3.0 nm for PD6,[23,24] and 4.5 nm for DPB determined by light-scattering experiments.[18,25] All the polysilanes prepared in the present study have high molecular weights ($>10^4$), low polydispersities (<4), and monomodal distributions similar to the Schulz−Zimm distribution. The polysilanes with high values of α such as DPB or PH5−PH12, expected to exhibit longer segment length, have molecular weights higher than 10^5. A flexible wormlike chain model with a persistence length of ∼10 nm successfully reproduced the global dimension of the Si chain in DPB with a molecular weight of $\sim 10^5$.[26] Thus, for almost all of the polysilanes in the present study, flexible Kuhn chains are acceptable as the first approximation model of their chain configurations on the basis of α and molecular weight. The gyration length of the flexible Kuhn chain is given by

$$R_g = \left(\frac{\langle r^2\rangle_0}{6}\right)^{1/2} \tag{3}$$

where $\langle r^2\rangle_0$ is the mean-square end-to-end distance observed in θ solutions. The value of q at the chosen molecular weight is derived from the mean-square end-to-end distance ($\langle r^2\rangle$) as follows:

$$q = \langle r^2\rangle\left(\frac{M_L}{2M}\right) \tag{4}$$

where M_L is the mass per unit length. The excluded volume parameter a is defined as $a^2 \equiv \langle r^2\rangle/\langle r^2\rangle_0$ and has been reported to be less than 1.2 for DPB at 25 °C in toluene, which is a better solvent than THF.[24] The low second virial coefficient of PD6 in THF (1.14×10^{-4} mL mol/g^2) also supports the small contributions of excluded volume effects on the conformations of polysilanes with longer segment lengths than PD6.[23,24] Thus, the assumption of $a = 1$ gives an appropriate estimate of the segment length for DPB, PH5−PH12, and PD6−PD12, although the segment length of polysilanes with highly flexible backbones may be underestimated. On the basis of the Si−Si bond length (0.2414 nm) and Si−Si−Si bond angle (114.4°),[27] the estimated Kuhn segment length varies from 0.55 to 8.6 nm (PH2−PH8) for the poly(*n*-alkylphenylsilane)s, 0.48−1.1 nm (ME3−ME10) for the poly(methyl-*n*-alkylsilane)s, and 2.4−6.3 nm (PD4−PD12) for the poly(di-*n*-alkylsilane)s.

The segment length also reflects the degree of delocalization of the lowest excitonic state along the Si chains and is described by the following empirical relationship:[9,18,28]

$$\epsilon_{abs} = 330 \cdot L \tag{5}$$

where L is the segment length in Si repeating numbers. Equation 3 gives a shortest value of $L \cong 13$ for PH2 and a longest value

(23) Cotts, P. M.; Ferline, S.; Dagli, G.; Pearson, D. S. *Macromolecules* **1991**, *24*, 6730.
(24) Shukla, P.; Cotts, P. M.; Miller, R. D.; Russel, T. P.; Smith, B. A.; Wallraff, G. M.; Baier, M.; Thiyagarajan, P. *Macromolecules* **1991**, *24*, 5606.
(25) Koe, J. R.; Fujiki, M.; Motonaga, M.; Nakashima, H. *Macromolecules* **2001**, *34*, 1082.
(26) Cotts, P.; Miller, R. D.; Sooriyakumaran, R. In *Silicon-Based Polymer Science: A Comprehensive Resource*; American Chemical Society: Washington, DC, 1990; Chapter 23, p 397.
(27) Koe, J. R.; Powell, D. R.; Buffy, J. J.; Hayase, S.; West, R. *Angew. Chem., Int. Ed.* **1998**, *37*, 1441.
(28) Schreiber, M.; Abe, S. *Synth. Met.* **1993**, *55−57*, 50.

of $L \cong \sim 53$ for PH8 in the present study, consistent with the changes in f_{VB-ES}.

In the pulse radiolysis experiment, the incident electron pulse in the solution produces radical cations ($Bz^{\bullet+}$), excited states (Bz*), and electrons as follows:

$$Bz \rightarrow Bz^{\bullet+}, Bz^*, e^- \quad (6)$$

The excited states and excess electrons are rapidly scavenged in oxygen-saturated solutions ($[O_2] = 11.9$ mM at 1 atm, 25 °C), giving singlet oxygen molecules ($^1O_2$) and oxygen anions (O_2^-).[29−31] Polysilanes (PS) in the solution react with $Bz^{\bullet+}$ via $Bz_2^{\bullet+}$, yielding polymer radical cations ($PS^{\bullet+}$):

$$Bz^{\bullet+} + PS \xrightarrow[k_1]{} Bz + PS^{\bullet+} \quad (7)$$

We have already discussed the transient spectra of radical ions of polysilanes, including PH1, PD6, etc.[12,18,21,29,32,33] $PS^{\bullet+}$ was found to exhibit two absorption bands in the near-UV (∼350−400 nm) and infrared (IR; >1600 nm) regions. The transient spectra of $PS^{\bullet+}$ suggest the presence of an interband level occupied by a hole (IBL^+). The UV and IR bands in $PS^{\bullet+}$ are due to transition from IBL^+ to the conduction band (CB) and from the valence band (VB) to IBL^+, respectively. The presence of IBL^+ is well interpreted as a delocalized positive polaron state[21,34−36] and/or Anderson localization state on an Si segment.[37,38] Figures 4−6 show a series of transient absorption spectra of radical cations observed in poly(*n*-alkylphenylsilane)s, poly(methyl-*n*-alkylsilane)s, and poly(di-*n*-alkylsilane)s, respectively. The spectra observed in Figures 5 and 6 are almost identical, with only a small dependence on the chain length of *n*-alkyl substituents. In contrast, poly(*n*-alkylphenylsilane)s in Figure 4 exhibit dramatic changes in the IR band with a considerable red-shift upon elongation of the *n*-alkyl chains. The peak energy of the IR band in relation to the binding energy of positive polarons on the Si chains[21,39] is given by:

$$\delta\epsilon \approx \left(\frac{\Delta V}{2A}\right)\left(\frac{a}{\xi_p}\right)^2 \quad (8)$$

where $\delta\epsilon$ denotes the binding energy of a polaron, a denotes a lattice unit of a trans-chain segment, and ξ_p is the polaron width. V is the matrix element describing the interaction between two atomic orbitals consisting of a covalent bond, and Δ denotes the matrix element between two atomic orbitals of an Si atom. The parameter A is given by

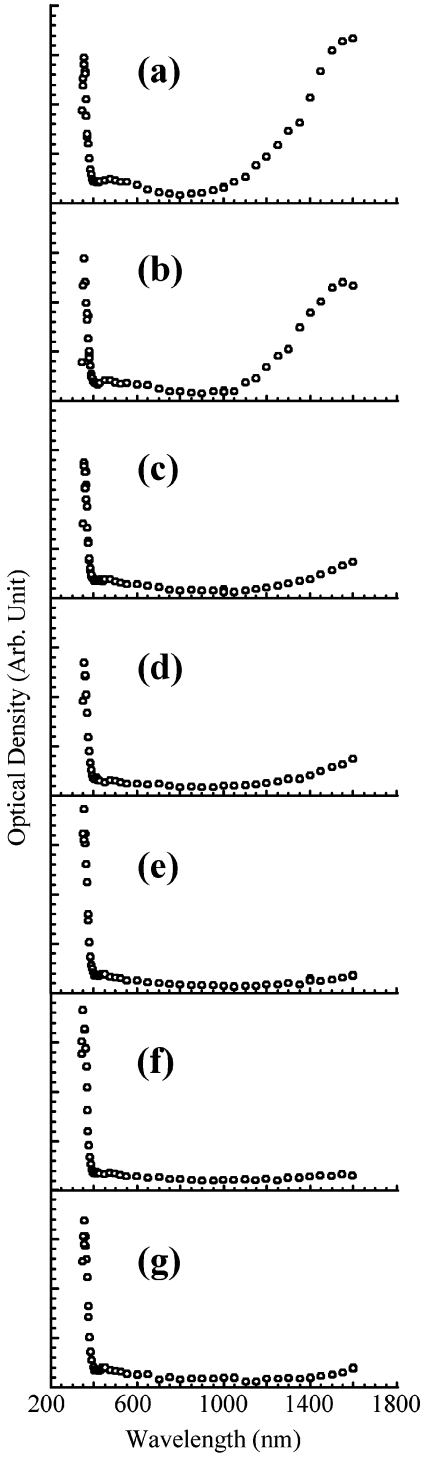

Figure 4. Transient absorption spectra of cation radicals of (a) PH1, (b) PH2, (c) PH5, (d) PH6, (e) PH8, (f) PH10, and (g) PH12 in Bz at 5.0×10^{-3} mol dm^{-3} (base mol unit). Spectra were observed for O_2-saturated solutions at room temperature, recorded 100 ns after electron pulse irradiation.

$$A \equiv [V(l) - \Delta]$$

$$l = \frac{a}{\sin\theta} \quad (9)$$

where 2θ is the tetrahedral bond angle. Thus, Δ is a parameter specifying the degree of delocalization of σ-electrons on a σ-conjugated segment, while V describes the localization of a pair of electrons in a local bond. The relative polaron width on

(29) Kawaguchi, T.; Seki, S.; Okamoto, K.; Saeki, A.; Yoshida, Y.; Tagawa, S. *Chem. Phys. Lett.* **2003**, *374*, 353.
(30) Candeias, L. P.; Wildeman, J.; Hadziioannou, G.; Warman, J. M. *J. Phys. Chem. B* **2000**, *104*, 8366.
(31) Grozema, F. C.; Siebbeles, L. D. A.; Warman, J. M.; Seki, S.; Tagawa, S.; Scherf, U. *Adv. Mater.* **2002**, *14*, 228.
(32) Seki, S.; Yoshida, Y.; Tagawa, S. *Radiat. Phys. Chem.* **2001**, *60*, 411.
(33) Seki, S.; Kunimi, Y.; Nishida, K.; Yoshida, Y.; Tagawa, S. *J. Phys. Chem.* **2001**, *B105*, 900.
(34) Rice, M. J.; Phillpot, S. R. *Bull. Am. Phys. Soc.* **1987**, *58*, 937.
(35) Abkowitz, M. A.; Rice, M. J.; Stolka, M. *Philos. Mag.* **1990**, *B61*, 25.
(36) Seki, S.; Yoshida, Y.; Tagawa, S.; Asai, K.; Ishigure, K.; Furukawa, K.; Fujiki, M.; Matsumoto, N. *Philos. Mag.* **1999**, *B79*, 1631.
(37) Ichikawa, T.; Yamada, Y.; Kumagai, J.; Fujiki, M. *Chem. Phys. Lett.* **1999**, *306*, 275.
(38) Ichikawa, T.; Sumita, M.; Kumagai, J. *Chem. Phys. Lett.* **1999**, *307*, 81.
(39) Pitt, C. G. In *Homoatomic Rings, Chains, and Macromolecules of Main Group Elements*; Rheingold, A. L., Ed.; Elsevier: Amsterdam, 1977.

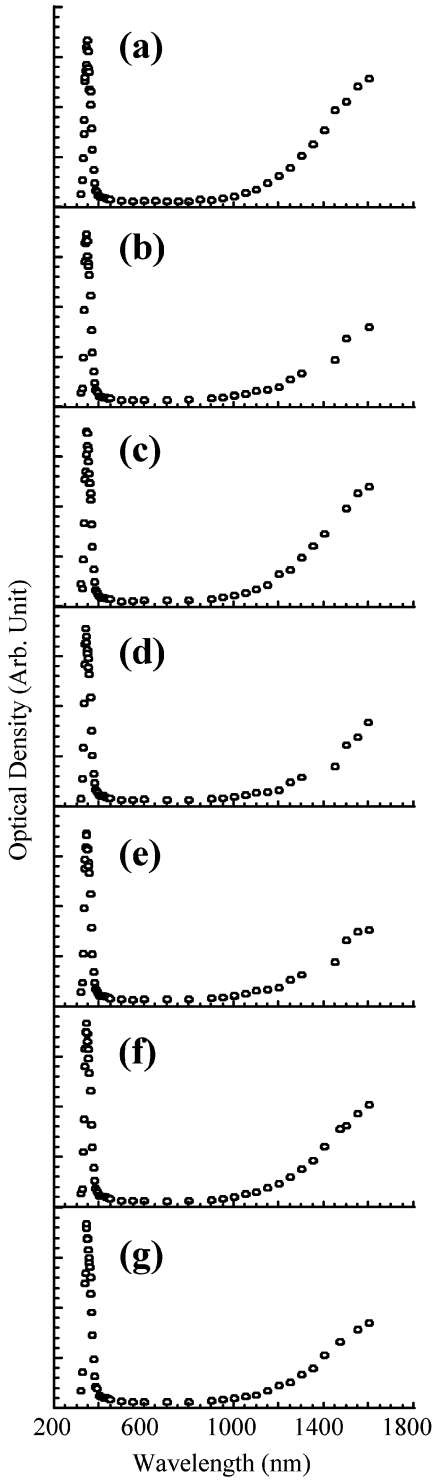

Figure 5. Transient absorption spectra of cation radicals of (a) ME3, (b) ME4, (c) ME5, (d) ME6, (e) ME8, (f) ME10, and (g) ME12 in Bz at 5.0×10^{-3} mol dm^{-3} (base mol unit). Spectra were observed for O_2-saturated solutions at room temperature, recorded 100 ns after electron pulse irradiation.

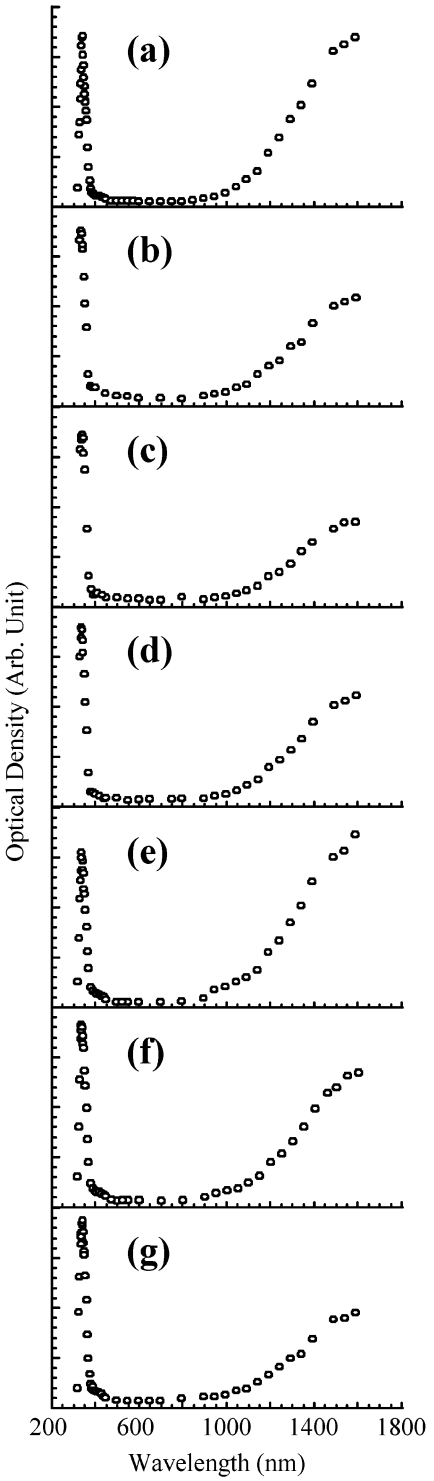

Figure 6. Transient absorption spectra of cation radicals of (a) PD4, (b) PD5, (c) PD6, (d) PD7, (e) PD8, (f) PD10, and (g) PD12 in Bz at 5.0×10^{-3} mol dm^{-3} (base mol unit). Spectra were observed for O_2-saturated solutions at room temperature, recorded 100 ns after electron pulse irradiation.

the polymers can be estimated based on eq 8. With the previously reported values of Δ in poly(dimethylsilane)[40,41] and V in poly(dichlorosilane),[27,41] the value of (ΔV/2A) can be estimated to be ca. 1.6 eV. The transition energy of the IR band observed for PH2 is 0.77 eV, the highest value for all the polysilanes, yielding $\xi_p = \sim 2$ Si repeating units as the minimum value. The considerable red-shift of the IR band observed for poly(*n*-alkylphenylsilane)s induces a dramatic increase in the polaron width and, hence, a highly delocalized positive charge state. Figure 7 shows the transient UV band observed for the ME3 solution. The spectra appear to suggest the simultaneous formation of the radical anion and cation in the Ar-saturated

(40) Kumada, M.; Tamao, K. *Adv. Organomet. Chem.* **1968**, *6*, 80.
(41) Pollard, W. B.; Lucovsky, G. *Phys. Rev. B* **1982**, *26*, 3172.

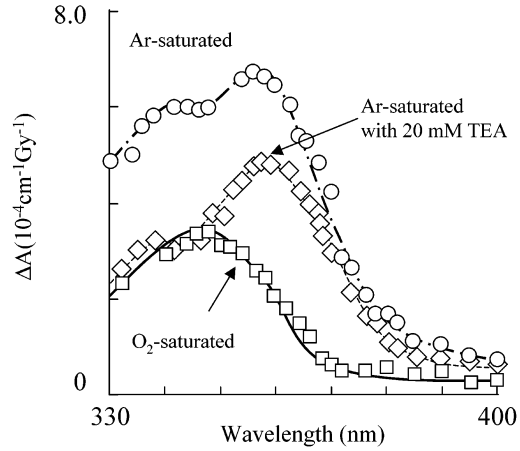

Figure 7. UV band in the transient absorption spectra of ME3 in Bz at 5.0×10^{-3} mol dm^{-3} (base mol unit). Spectra were recorded 100 ns after electron pulse irradiation. Solid (□), dashed (◇), and dot−dashed (○) lines are spectra observed in O_2-saturated and Ar-saturated with TEA at 2.0×10^{-3} mol dm^{-3} and Ar-saturated solutions, respectively.

solution, leading to overlap of the two transient absorption bands at 358 and 348 nm, which have been determined independently in previous work.[29,32,33] In contrast to the Ar-saturated solution, only the radical anion or the radical cation is selectively formed in the Ar-saturated solution with 20 mM triethylamine (TEA) or the O_2-saturated solution. The kinetic trace is recorded over a wide range of observation time from a few nanoseconds to microseconds. The extinction coefficient of the radical cations can be determined by the charge-transfer reaction between $PS^{\bullet+}$ and TMPD as follows:

$$PS^{\bullet+} + TMPD \xrightarrow[k_3]{} TMPD^{\bullet-} + PS \qquad (8)$$

However, $TMPD^{\bullet+}$ is also formed by direct reaction with $Bz^{\bullet+}$, i.e.:

$$Bz^{\bullet+} + TMPD \xrightarrow[k_2]{} Bz + TMPD^{\bullet+} \qquad (9)$$

$ME3^{\bullet+}$ and $TMPD^{\bullet+}$ decay primarily via second-order reactions with O_2^- as follows:

$$PS^{\bullet+} + O_2^- \xrightarrow[k_4]{} PS, O_2, \text{oxidized polymers} \qquad (10)$$

$$TMPD^{\bullet+} + O_2^- \xrightarrow[k_5]{} TMPD, O_2, \text{products} \qquad (11)$$

The formation process of $TMPD^{\bullet+}$ can be observed as an increasing process in the transient absorption at 570 nm, at which $TMPD^{\bullet+}$ in Bz peaks with an extinction coefficient of 1.2×10^4 M^{-1} cm^{-1}.[20] Figure 8 shows the formation kinetics of $TMPD^{\bullet+}$ at 570 nm and the decay process of $ME3^{\bullet+}$ at 348 nm by the addition of TMPD. The values of k_1, k_2, and k_3 are estimated to be 5.6×10^9, 3.2×10^9, and 1.8×10^{10} M^{-1} s^{-1} for ME3. The kinetic trace observed for $ME3^{\bullet+}$ in the presence of TMPD is well fitted by a simulation on the basis of these k_1, k_2, and k_3 values and the assumption of $k_{4-5} \approx 10^5$ M^{-2} s^{-1}, with only minor disagreement in the longer time region. The fitting of the trace based on the extinction coefficient of $TMPD^{\bullet+}$ gives $PS^{\bullet+}$ extinction coefficients ($\epsilon^{\bullet+}$) of 3.3×10^4 to 2.0×10^5 M^{-1} cm^{-1}, as listed in Table 2. The initial free ion yield in benzene ($G(Bz^+)$) is estimated to be $G(Bz^+) = 0.050 \pm 0.004$, which is in good agreement with the previously reported value.[42]

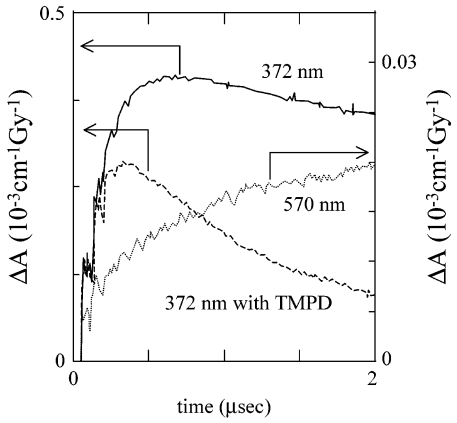

Figure 8. Kinetic traces of ME3 cation radicals in O_2-saturated Bz at 5.0×10^{-3} mol dm^{-3} (base mol unit). Traces are observed at 348 nm (solid: ME3 only, dashed: ME3 with TMPD at 0.19×10^{-3} mol dm^{-3}) and 570 nm (dotted: ME3 with TMPD at 0.19×10^{-3} mol dm^{-3}).

In the quantitative elucidation of the degree of charge delocalization on the Si skeleton, we have already reported the degree of charge delocalization (n_{del}) determined through simultaneous observation of the transient bleaching of the lowest excitonic backbone peak (Δ_{OD}^{Bl}) and the formation of the UV bands ($\Delta_{OD}^{\bullet\pm}$), as given by[18,32]

$$n_{del} = \frac{\Delta_{OD}^{Bl} \cdot \epsilon^{\bullet\pm}}{\Delta_{OD}^{\bullet\pm} \cdot \epsilon_{ES}} \qquad (12)$$

The empirical relationship between the apparent oscillator strength of the UV band ($f^{\bullet\pm}$) and the value of n_{del} has also been obtained, expressed as:[18,33]

$$n_{del} \propto f^{\bullet\pm} \qquad (13)$$

$$f^{\bullet\pm} = 4.32 \times 10^{-9} \int \epsilon^{\bullet\pm} \, d\nu \qquad (14)$$

The values of $f^{\bullet+}$ can be obtained by numerical integration of the Gaussian fit to the IBL^+−CB transitions. The obtained values of $f^{\bullet+}$ are also summarized in Table 2. The half-Gaussian (high-energy side), half-Lorentzian (low-energy side) fit gives lower values of $f^{\bullet+}$, but the difference between the two fittings is less than 20% for all spectra. The values of $f^{\bullet+}$ for a series of poly(dialkylsilane)s, poly(*n*-alkylphenylsilane)s, and poly(arylsilane)s are plotted as a function of α in Figure 9. The values of $\epsilon^{\bullet+}$ principally reflect the values of α and exhibit a similar dependence on the degree of delocalization of excitonic states on the Si backbone. However, $\epsilon^{\bullet+}$ and $f^{\bullet+}$ values observed for the phenyl-substituted polysilanes are clearly higher than those for the dialkyl-substituted polysilanes.

The values of both *q* and *L* derived from eqs 4 and 5 clearly indicate that the physical segmentation length in Si backbones of the ground-state or excited-state polysilanes is well interpreted in terms of molecular stiffness α. In the case of radical cations, the dependence of $f^{\bullet+}$, or n_{del}, on molecular stiffness can be apparently categorized into three series: polysilanes bearing no, one, or two phenyl rings. It should be noted that the transient spectra in the present study were recorded after intrachain charge-transfer processes, which were expected to occur within a few nanoseconds;[43] thus, the spectra are mainly due to

(42) Gee, N.; Freeman, G. R. *Can. J. Chem.* **1992**, *70*, 1618.

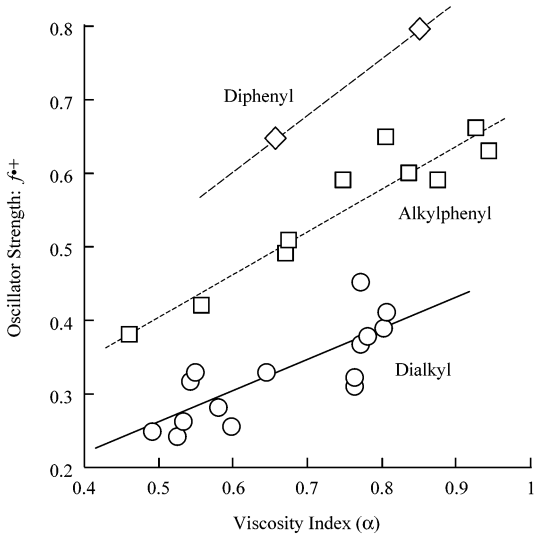

Figure 9. Oscillator strength ($f^{\bullet+}$) of UV band vs viscosity index (α).

energetically favorable segments in polysilane backbones. Despite the fact that PH2 exhibit almost identical Stokes shifts to those of any poly(dialkylsilanes), a relatively high value of $f^{\bullet+}$ is observed for PH2. This is strongly suggestive of a crucial contribution from the phenyl rings in the delocalization of positive charges. Takeda et al. suggested that, on the basis of theoretical calculations, the valence and excitonic states of steady-state polysilanes bearing phenyl rings are considerably affected by $\sigma-\pi$ mixing.[44] The present results also indicate that this is the case, giving rise to IBL^+. A delocalized IBL^+ over the phenyl ring is a good explanation for the increase in $f^{\bullet+}$ for poly(*n*-alkylphenylsilane). This explanation is supported by models of the spread of the singly occupied molecular orbital (SOMO) state into substituents, as calculated theoretically for polysilane radical cations.[14,37] Therefore, the UV band includes both the transition from IBL^+ to the CB and the transition from IBL^+ to pseudo-π at an energy of ~0.2 eV below the CB.

Conclusion

The molar extinction coefficients of radical cations were examined quantitatively for a variety of substituted polysilanes. On the basis of a charge-transfer reaction between $PS^{\bullet+}$ and TMPD, the extinction coefficients of $PS^{\bullet+}$ ($\epsilon^{\bullet+}$) were estimated to be 3.3×10^4 to $>2.0 \times 10^5$ M^{-1} cm^{-1}. The values of $\epsilon^{\bullet+}$ principally reflect the values of α and exhibit a similar tendency to the degree of delocalization of the excitonic state on the Si backbone. The observed values of $\epsilon^{\bullet+}$ and $f^{\bullet+}$ for phenyl-substituted polysilanes were significantly higher than those for dialkyl-substituted polysilanes. A contribution by $\sigma-\pi$ mixing effects in polysilanes bearing phenyl rings readily explains the higher oscillator strength in poly(*n*-alkylphenylsilane)s and poly(diarylsilane)s.

Acknowledgment. We acknowledge Prof. M. Fujiki of Nara Institute of Science and Technology (NAIST), Graduate School of Material Science, and Prof. J. R. Koe of Department of Chemistry, International Christian University for supplying DPA and DPB. We thank Dr. Y. Kunimi, Mr. Suemine, and Mr. T. Yamamoto of the ISIR, Osaka University for experimental support. This work was supported in part by a grant-in-aid for scientific research from the Japan Society for the Promotion of Science.

JA039840E

(43) Matsui, Y.; Nishida, K.; Seki, S.; Yoshida, Y.; Tagawa, S.; Yamada, K.; Imahori, H.; Sakata, A. *Organometallics* **2002**, *21*, 5144.
(44) Matsui, Y.; Seki, S.; Tagawa, S. *Chem. Phys. Lett.* **2002**, *357*, 346.
(45) Takeda, K.; Teramae, H.; Matsumoto, N. *J. Am. Chem. Soc.* **1986**, *108*, 8186.